

Model and test of a modular inspection robotic system

A. Aluței*, M.O. Tătar**, C. Cirebea***

*Technical University of Cluj-Napoca, Memorandumului 28, 400114 Cluj-Napoca, Romania,
E-mail: adrian.alutei@mmfm.utcluj.ro

**Technical University of Cluj-Napoca, Memorandumului 28, 400114 Cluj-Napoca, Romania,
E-mail: olimpiut@yahoo.com

***Technical University of Cluj-Napoca, Memorandumului 28, 400114 Cluj-Napoca, Romania,
E-mail: claudiu.cirebea@mmfm.utcluj.ro

1. Introduction

Inspection robotics is one of the most important branches in the robotics field due to its many applications into pipe, mining and petroleum sites inspection industry. Mobile inspection robots can inspect places which are hazardous and/or inaccessible to humans [1-3]. These robots are modular systems and they have several interchangeable (active and passive) modules and they are using different locomotion methods. The control of the robotic systems is done from a distance. The main advantages of these modular systems are versatility, simplicity, robustness and low cost of fabrication.

2. Proposed active and passive robotic module

The active module of the robotic system consists of the actuator, transmission system (from the actuator to the wheels) and six independent sliding mechanisms, positioned two by two at 120° angles around the longitudinal axis of the module. The wheels of the active module are pressed against the inner surface of the inspected pipe using two compression springs placed one on each side of the module's central axle.

The 3D detailed model of the suggested robotic system is presented in Fig. 1.

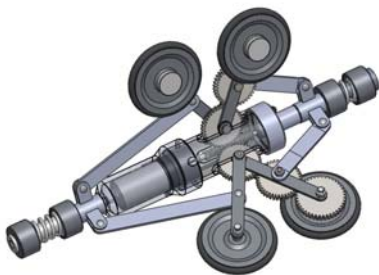


Fig. 1 The 3D model of the active inspection module

The passive module has the task of transporting the electronic equipment and the batteries that power the actuators. It has a cylindrical shape and six wheels, three at each end of the module, placed at 120° angles around the longitudinal axis.

The axle of each individual wheel is mounted in a fork-like clamping system which is placed on a rod with a compression spring that allows the wheel to slide along an axis that is perpendicular on the longitudinal axis of the module. In this way the module can cross sections of pipes with different diameters. The 3D model of the passive module is presented in Fig. 2.

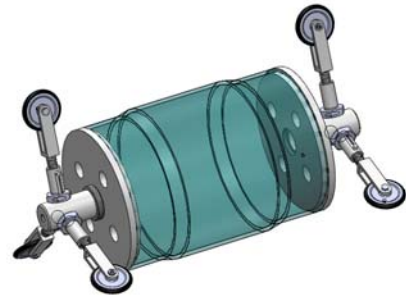


Fig. 2 The 3D model of the passive inspection module

3. Active robotic module

The actuator is positioned in the centre of the active module and the transmission is done through a worm-gear mechanism. The transmission system is composed of the following elements: 1 – single-enveloping worm ($z_1 = 1$, module $m = 0.75$ mm, angle of the worm spiral $\theta = 4^\circ$); 2, 3, 4 – gears with angled teeth (teeth angle is $\beta = 4^\circ$); $z_2 = 42$, $z_3 = 38$, $z_4 = 38$ – number of teeth (Fig. 3).

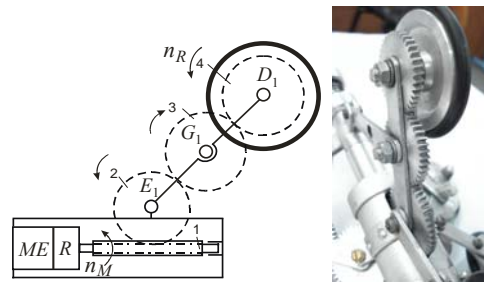


Fig. 3 Movement transmission from the actuator to the active wheel

For the development of the mathematical model, the following annotation were made: \bar{F}_f as the friction force between the wheel and the pipe wall, $F_f = \mu F_R$, where \bar{F}_R is the reaction force between the wheel and the pipe wall; \bar{M}_{fr} as the rolling friction torque $M_{fr} = s_f \cdot F_R$, where s_f is the rolling friction coefficient; μ as the slip friction coefficient; ω_R as the angular speed of the wheel; d as the diameter of the wheel axle; k as the active module's springs constant; R as the active and passive wheel's radius; v as the robot's speed $v = \omega_R R$; G as the weight force of the active module; m_1 as the actual mass of the

active module; $M_{r\text{ax}RM}^r$ represents the resistant reduced torque of the actuator's axle; M_{fl} represents the friction torque in the wheel bearing and has the expression

$$M_{fl} = \frac{\mu d F_R}{2} \quad (1)$$

The considered mass of the active module is $m_1 = 630$ g, the elements have the lengths $h_1 = 95$ mm, $h_2 = 58$ mm, $h_3 = 53$ mm, the radius of the wheels $R = 25$ mm. The mechanism in one plane projection of the active module is presented in Fig. 4.

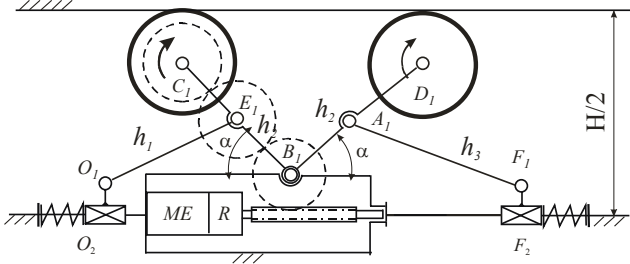


Fig. 4 Mechanism of the active module

The angle α that appears between the horizontal axle O_2F_2 and $h_2/2 = E_1B_1$ for the left arm and $h_2/2 = B_1A_1$ for the right arm; it has a determined variation that ranges between 25 and 50°. From the 3D model we can determine the maximum and minimum height of the robot, based on the movement of the mechanisms and on the variation of angle α . Eq. (2) represents the variation of one arm; the distance between O_1 and O_2 was noted a

$$H / 2 = R + a + h_2 \sin \alpha \quad (2)$$

Eq. (2) doesn't take into consideration the presence of the springs, but only the positions of the elements in respect with the variation of α angle. Fig. 5 presents the variation of the height of the active module in respect with α angle.

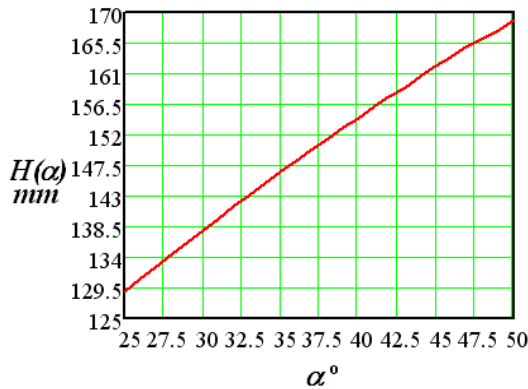


Fig. 5 Height of the active module as a function of the angle α

If we take the spring into consideration and we want to determine the dependence between the spring force and the reaction force, based on the mechanism from Fig. 2, the following equations are used for each of the two active arms in the active module

$$F_{R1} = k \Delta x_1 \operatorname{tg} \alpha \quad (3)$$

$$F_{R2} = k \Delta x_2 \operatorname{tg} \alpha \quad (4)$$

For determining the resistant torque reduced in the actuator axle, the vertical movement position of the robotic system inside a pipe was taken into consideration.

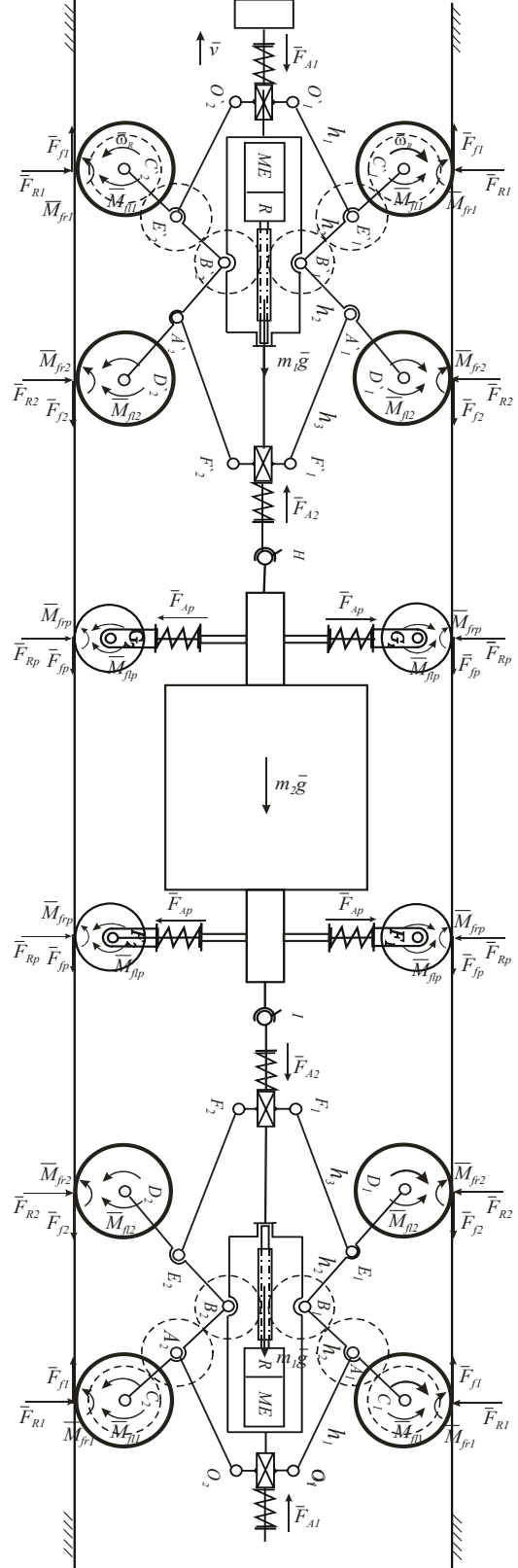


Fig. 6 Force and momentum distribution in the modular system

Fig. 6 presents the force distribution scheme and the parameters of the whole robotic system in case of vertical movement inside a pipe.

$$M_{r_{axM}}^r = \frac{1}{i_{reducer} i_{transmission}} \left[3F_{R1} \left(s_f + \frac{\mu d}{2} \right) + Rm_1 g + 3F_{R2} \left(s_f + \frac{\mu d}{2} \right) + \frac{1}{2} Rm_2 g + 3k_2 \Delta x_p \left(s_f + \frac{\mu d}{2} \right) \right] \quad (5)$$

The calculated value for the reduced torque at the axle of the actuator is $3.5 \cdot 10^{-4}$ Nm.

4. Model of the driving system

The actuator used for the active module is positioned in the centre of the system; it is a geared DC motor with a transmission ratio of $i_{reducer} = 19$. In order to select a proper actuator that will fit the required dimensions, power consumption and torque, the Matlab/Simulink model of the DC motor will be developed.

The DC motor model was obtained using the transfer function starting from the following electrical and mechanical equations

$$\begin{cases} u_A - e = R_A i_A + L_A \frac{di_A}{dt} \\ e = K_e \omega_m \end{cases} \quad (6)$$

$$\begin{cases} M_m = I^r \varepsilon + K_d \omega_m + M_r^r \\ M_m = K_m i_A \\ M_r^r = \frac{1}{i_{total}} M^r \\ I^r = I_m + \frac{1}{(i_{total})^2} I_R \end{cases} \quad (7)$$

where u_A represents the input voltage, R_A is the electric resistance, i_A is the armature current, e is the counter-electromotive force, L is the electric inductance, K_m motor torque constant, K_e ($K_m = K_e$) electromotive force constant, $K_d \omega_m$ ($K_d = b$) damping torque given by the loss of magnetic field and viscous friction in the motor's bearings, M_m is the motor's torque, M_r^r is the resistant torque reduced in the axle of the motor, I^r is the moment of inertia of the rotor and $i_{total} = i_{reducer} i_{transmission}$.

Applying the Laplace transformation on Eqs. (6), (7) and considering the resistant torque $M^r = 0$, the transfer function is obtained

$$\frac{\Omega_m(s)}{U_A(s)} = \frac{K_m}{(I^r s + K_d)(L_A s + R_A) + K_e K_m} \quad (8)$$

The equivalent scheme of the DC motor, based on Eq. (8) and the Matlab Simulink model is presented in Fig. 7.

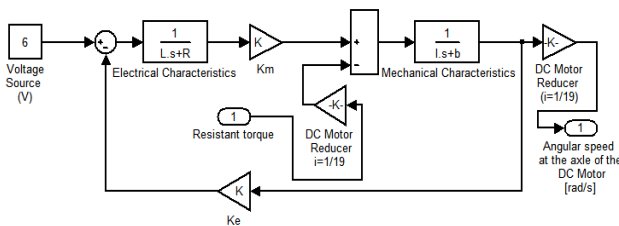


Fig. 7 Actuator model

Based on the scheme in Fig. 6, the equation of the reduced torque in the actuator's axle will be

The transmission model takes into consideration the relation $\omega_{out} = \frac{z_1}{z_4} \cdot \omega_{in}$, between the angular speed at the

entrance of the transmission and the output angular speed. The reduced torque from the wheel in the motor axle is multiplied with $1/i_{transmission}$ (Fig. 8), where $i_{transmission}=38$ represent the transmission ratio

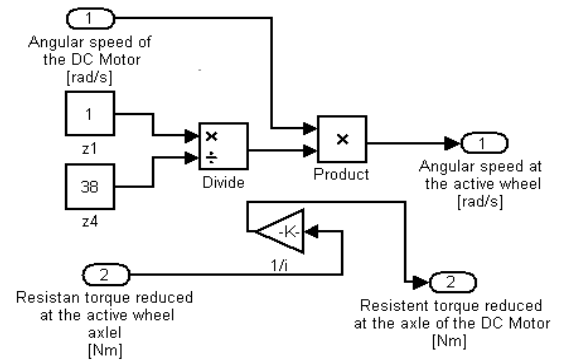


Fig. 8 Transmission model

The final model of the driving system is presented in Fig. 9.

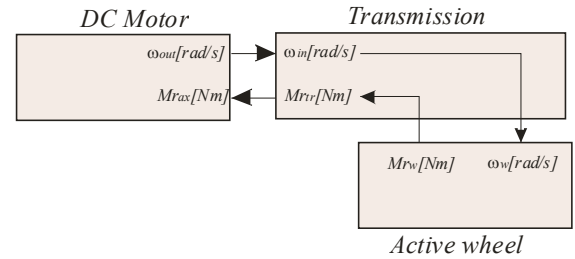


Fig. 9 Matlab/Simulink model of the driving system

In conditions of pure rolling, the motor output power P_m is presented as a function of traction force $F_{traction}$, wheels speed $v_w = \omega_i \cdot R$ and motor efficiency η .

$$P_m = F_{traction} \frac{v_w}{\eta} \quad (9)$$

The traction force for the active module is

$$F_{traction} = \frac{M_m i_{total} \eta}{r_{wheel}} \quad (10)$$

After the simulation, the best results were obtained by the IG 22 series motor, which had the following output data: $b = 2.6 \cdot 10^{-6}$ Nm/rad/s; $K_e = 5.7 \cdot 10^{-3}$ Nm/A; $R_A = 3 \Omega$; $L = 6$ mH and $I^r = I = 1.5 \cdot 10^{-6}$ kgm². At a voltage supply of 6 V, the torque in the axle of the motor was $M = 1.768 \cdot 10^{-3}$ Nm. For the active wheel the number of revolutions was $n = 11.219$ rpm, and the torque of the ac-

tive wheel was $M = 1.277$ Nm. The condition that requires the torque of the motor to be higher than the reduced torque at the axle of the motor is done.

5. The developed prototype of the inspection robotic system

A prototype of the suggested system was developed and tested. Fig. 10 presents the 3D design and the developed prototype picture.

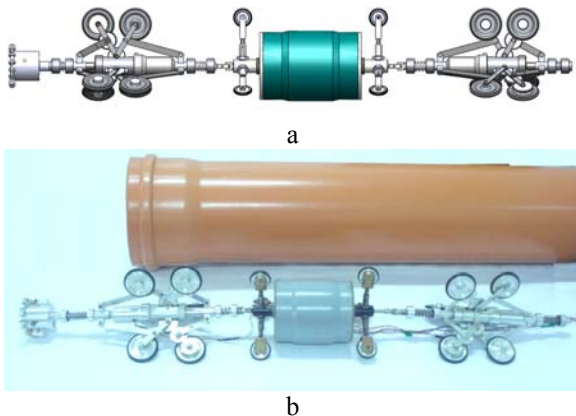


Fig. 10 3D design (a) and the developed prototype (b)

The prototype is able to inspect pipes with the interior diameter ranged between 130 and 170 mm. It weights 1980 g and has a length of 856 mm. The force exerted on the inner pipe walls for all prototypes is generated with the help of a compression spring. The springs placed on the central axis assure the repositioning of the structure in the event of pipe diameter variation. The joint element placed between the modules is a universal joint and it helps the modules to orientate easily in the environment. The inspection robotic system that was developed was tested into horizontal pipes. The cable influence on the movement inside the pipe was not taken in consideration because the robotic system has the capability to be autonomous energetically. The system's speed inside the pipe was of 150 mm/s at 6 V supply voltage. A wireless mini-camera was mounted on the front end of the robotic system for inspection purposes.

6. Acknowledgment

This work is supported by the CNCSIS (National Council of Scientific Research in Higher Education from Romania); through PNII - IDEI Project, ID_1056: Modeling, simulation and development of robotic system families used for inspection and exploration.

References

1. **Choi, H.R., Ryew, S.M.** Robotic system with active steering capability for internal inspection of urban gas pipelines. -Mechatronics, 2002, vol.12, p.713-736.
2. **Roh, S.G., Choi, H.R.** Differential-drive in-pipe robot for moving inside urban gas pipelines, IEEE Transactions Robotics, 2005, vol.21, No.1, p.1-17.
3. **Nitulescu, I M., Stoian, V.** Modelling and control aspects of specific mobile robot. -Mechanika. -Kaunas:

Technologija, 2008, Nr.1(69), p.54-58.

4. **Abdelbaki, N., Bouali, E., Gaceb, M., Bouzid, R.** Influence of properties of large pipes on the reliability of pipelines. -Mechanika. -Kaunas: Technologija, 2008, Nr.1(69), p.19-23.
5. **Tătar, M.O., Aluței, A., Mândru, D.** Driving module for modular robotic system, vol. Machine Design 2009, Ed. S. Kuzmanovic, University of Novi Sad, 2009, p.147-150.
6. **Tătar, M.O., Aluței, A., Mândru, D.** In pipe modular robotic systems for inspection and exploration. Solid State Phenomena Vol. 164 (2010), Trans Tech Publications, Switzerland, p 425-430

A. Alutei, M.O. Tatar, C. Cirebea

PAIEŠKOS MODULINĖS ROBOTIZUOTOS SISTEMOS MODELIS IR JO TYRIMAS

Reziumė

Šio straipsnio tikslas pristatyti autorių sukurtos aktyvios paieškos robotizuotos sistemos matematinį modelį ir jo imitaciją. Naudojantis imitavimo rezultatais buvo nustatyta didžiausia erdvė, kurioje robotas gali veikti, pavarų, kurios gali būti panaudotos tipai, ir valdymo sistema, turinti įtakos roboto projektavimui.

A. Aluței, M.O. Tătar, C. Cirebea

THE MODEL AND SIMULATION OF AN INSPECTION ROBOTIC SYSTEM

Summary

The aim of the paper is to present the mathematical model and the simulation for an active robotic inspection system developed by the authors. Based on the results of the simulation, important data was acquired regarding the maximum space in which the robot can operate the type of actuators that should be used and the design of the control system, which influenced the development of the robot.

A. Алутэи, М.О. Татар, Ц. Циребеа

МОДЕЛЬ И ИССЛЕДОВАНИЕ МОДУЛЬНОЙ РОБОТИЗИРОВАННОЙ ПОИСКОВОЙ СИСТЕМЫ

Резюме

Цель статьи – представление созданной авторами математической модели активной роботизированной системы и ее имитация. При использовании результатов имитации определено максимальное пространство работы робота, типы используемых механизмов и системы управления, которая влияет на процесс проектирования робота.

Received May 07, 2010

Accepted August 27, 2010